JOURNAL OF Applied Polymer SCIENCE

Structure-Specific Sorbent Based on Nanostructures for Selective Recognition of Cimetidine from Its Structural Analogues

M. P. Sooraj, Beena Mathew
School of Chemical Sciences, Mahatma Gandhi University, Kottayam 686560, India
Correspondence to: B. Mathew (E-mail: beenamscs@gmail.com)

ABSTRACT: Synthetic molecular units for cimetidine recognition (MWCNT-MIP) were fabricated at the vinyl functionalized surface of MWCNT (MWCNT-CH=CH_2). The products and intermediates were characterized using Fourier-transform infrared spectroscopy, PXRD, thermogravimetric analysis, scanning electron microscope, and tunneling electron microscope techniques. The well fit curve of Langmuir adsorption isotherm clearly indicated the increased homogeneity of MWCNT-MIP ($R^2 = 0.998$) as compared to the bulk MIP ($R^2 = 0.966$). The rebinding process was found to follow a second-order kinetics with a rapid adsorption rate and decreased time period which suggested the enhancement of recognition sites on the surface of MWCNT-MIP. The maximum saturated binding capacity (Q_{max}) showed a 31.73% increase after the incorporation of MWCNT on MIPs. The relative selectivity coefficient (k') of MWCNT-MIP (6.82) was higher than that of the bulk MIP (4.23). In addition, reusability of bulk and MWCNT-MIPs was demonstrated. It was found that MWCNT-MIP showed five repeated cycles without any loss in performance. © 2014 Wiley Periodicals, Inc. J. Appl. Polym. Sci. **2014**, *131*, 40947.

KEYWORDS: adsorption; morphology; thermogravimetric analysis

Received 19 March 2014; accepted 1 May 2014
DOI: 10.1002/app.40947

INTRODUCTION

Molecular imprinting is the three-dimensional imprints of a target molecule in a rigid polymeric matrix built with synthetic materials made from vinyl functional derivatives.[1] The target molecule is later removed without disturbing the geometry of the solid matrix. The use of a suitable cross-linker also helps to maintain the rigidity of the polymer and its well defined recognition sites.[2] The molecularly imprinted polymer retains the ability to rebind the template because of its functional arrangement regarding shape selectivity and pre-organization of functional groups.[3] The main challenges to traditional bulk imprinting are deeply imprinted cavities, production of heterogeneous binding sites, entrapment of template molecules in the polymer matrix leading to poor site accessibility, etc.[4] This hinders the performance of the MIPs thus reducing the kinetics of binding target analyte. The development of nanotechnology has offered an opportunity to solve these problems because of the unique characteristics of nanometerials. Among them, the incorporation of CNTs into the polymer matrix has proven quite successful due to the increase in imprinted cavities within the polymer network owing to the high surface-to-volume ratio of MWCNT.[5] Binding polymers to CNTs is a very enticing area, because the individual properties of the two materials can be combined to give one hybrid material. MWCNTs are ideal support materials for MIPs because of their strong interactions, stability under acidic conditions and large surface area. Here the imprinted polymers wrap around the CNTs and eventually, most of the cavities are near or in the surface, with most template molecules being removed from the highly cross-linked matrix. In recent decades, molecularly imprinted polymer-CNT composite materials have attracted much attention for their potential applications in the fields of separation science,[6,7] sensing,[8,9] drug delivery, etc.[10] The effective utilization of CNTs in nanocomposite applications depends strongly on the ability to disperse the CNTs homogeneously throughout a matrix without destroying the integrity of the CNTs. So to improve the solubility and surface functionality, attention has been focused on their functionalization and surface modification.[11]

Cimetidine (CIM) is a histamine H_2-receptor antagonist that inhibits stomach acid production. Mainly it is used in the treatment of heartburn, peptic ulcers, gastric,[12] and breast cancer.[13] Many methods are available for the detection and characterization of CIM from its structurally related compounds. We present here an effective and efficient nanostructure-based sorbent technique for the selective recognition and separation of CIM from its structural analogues. The molecularly imprinted sorbent was prepared on vinyl functionalized multiwalled carbon nanotubes with CIM as template, acrylamide as functional monomer, EGDMA as

© 2014 Wiley Periodicals, Inc.

cross-linker and AIBN as initiator. Various parameters affecting the rebinding process were optimized. Then, the selective recognition of MWCNT-MIP/MIP towards the target molecule was evaluated using adsorption experiments. The adsorption isotherms and adsorption kinetics of the MWCNT-MIP were also studied in detail. The composition of MWCNT-MIP was analyzed using Fourier-transform infrared (FT-IR), powder XRD and thermo gravimetric analysis and their morphologies were observed using scanning electron microscopy and TEM (tunneling electron microscope) techniques.

EXPERIMENTAL

Materials

Pristine MWCNTs were purchased from Reinste Nano Ventures Private Limited,India. Acrylamide (AAm, 98%), 2-hydroxy ethyl methacrylate(HEMA 99%), ethylene glycol dimethacrylate (EGDMA, 98%) and all solvents (HPLC grade) were obtained from Merck, India. CIM (99%), Ranitidine (RAN, 99%), Famotidine (FAM, 99%), 2,2′-azo-bisisobutyronitrile (AIBN), and thionyl chloride ($SOCl_2$) were obtained from Sigma Aldrich. All chemicals and solvents were used without further purification.

Apparatus

The FT-IR spectra were recorded on a Perkin-Elmer 400 FT-IR spectrophotometer. Ultraviolet–visible (UV–vis) absorption spectra were investigated by a Shimadzu UV–vis. spectrophotometer model 2450. Thermogravimetric analysis (TGA) was conducted on a NETZSCHSTA449C instrument from room temperature to 800°C at a uniform heating rate of 10°C/min. Morphological images of MWCNT and modified MWCNT were recorded on a JEOL-JSM-6390A scanning electron microscope (SEM) and JEOL-2100 model TEM.

Purification of Pristine MWCNT

The purchased MWCNT was purified as reported elsewhere.[14] Briefly, the pristine MWCNT was heated in an air oven at 650°C for 2.5 h and then allowed to cool followed by the treatment with HCl for 1.5 h. The mixture of nanotube along with acid was diluted with deionized water and the resultant suspension was centrifuged (1400 rpm) to get the solid. It was then repeatedly washed with deionized water to make the pH around 7. The solid substance was filtered and dried in a vacuum oven for 9 h at 45°C.

Carboxyl Functionalization of MWCNT

To 0.75 g purified MWCNT taken in a round bottom flask, 50 mL conc. HNO_3 was added followed by sonication for about 12 minutes in a bath type sonicator at 40 kHz. The reaction flask was then put in to an oil bath maintained at 80°C equipped with a reflux condenser for 7.5 h under vigorous stirring. The mixture was then diluted with excess amount of deionized water and filtered through 0.2 μm PTFE membrane to separate the solid component. The washing procedure was repeated until the pH of the filtrate became neutral. The obtained solid product was dried under vacuum at 60°C for 24 h, yielding MWCNT with carboxyl functionalization. The distribution of surface acid functionalization groups was determined by Boehm titration method.[15]

Preparation of Vinyl Functionalized MWCNT (MWCNT-CH═CH_2)

About 0.5 g of MWCNT-COOH and 20 mL of $SOCl_2$ in 15 mL THF were taken in a reaction flask equipped with reflux condenser. The reaction mixture was refluxed at 65°C for 24 h under vigorous stirring. After cooling, the mixture was repeatedly washed with THF (5 × 25 mL). The solid product was separated from THF solution through centrifugation at 14,000 rpm which was then dried under vacuum at 60°C for 18 h. Surface vinyl functionalization of the obtained MWCNT-COCl was then carried out using 3 mL 2-hydroxy ethylmethacrylate yielding MWCNT-CH═CH_2.[16]

Preparation of CIM Molecularly Imprinted Polymer on MWCNT

About 0.075 g of vinyl functionalized MWCNT was mixed with 0.5 mmol of acrylamide (AAm), 0.1 mmol CIM, and 1 mmol EGDMA in a reaction vessel equipped with a reflux condenser containing 25 mL acetonitrile. The mixture was sonicated for 20 min for better dispersion. To this 50 mg AIBN was added and refluxed at 70°C for 24 h under N_2 atmos. After the completion of the reaction, the polymer was separated and ground well. It was then washed repeatedly with acetonitrile for the complete removal of drug molecules (Figure 1) which was monitored using UV–vis spectroscopy ($\lambda_{max} = 220$ nm). The obtained polymer was dried in a vacuum desiccator for 24 h before use. For comparison, the nonimprinted polymers on MWCNT (MWCNT-NIP) were also prepared using the same procedure, but without using the drug molecules in the polymerization process. Further the conventional bulk MIPs/NIPs were prepared following the above scheme but in the absence of MWCNT (Table I).

Adsorption Concentration

To optimize the concentration parameter, 0.01 g of MWCNT-MIPs/NIPs were treated with 8 mL of CIM solution having varying concentration (0.4–3.6 mmol L^{-1}) followed by equilibration in a shaken bed. From the collected centrifugate the concentration at which maximum amount of CIM bound by the polymer is determined using the following equation:

$$Q_e = (C_o - C_e)V/M \quad (1)$$

where C_o (mmol L^{-1}) and C_e (mmol L^{-1}) are the initial and equilibrium concentrations, V (L) is the volume of CIM solution and M (g) is the weight of the sorbent. The experiment was repeated for bulk MIPs/NIPs also.

Study on the Effect of Mass of Sorbent

Different weights (5, 10, 15, and 20 mg) of MWCNT-MIP/NIP and bulk MIP/NIP as well were shaken with the optimum concentration of the CIM solution (2.4 mmol L^{-1}) for 4 h. The amount of CIM bound by the polymer and its nano counterpart was calculated as mentioned in the concentration study.

Adsorption Experiment

Ten milligrams of the synthesized sorbents (MWCNT-MIP/MIP) was added to 8 mL each of template solution having different concentrations ranging from 0.4 to 2.4 mmol L^{-1}. It was then shaken for 4 h. The equilibrated mixture was centrifuged and decanted. Using UV–vis absorption at 220 nm, concentration of the supernatant liquid was estimated. From this data the adsorption

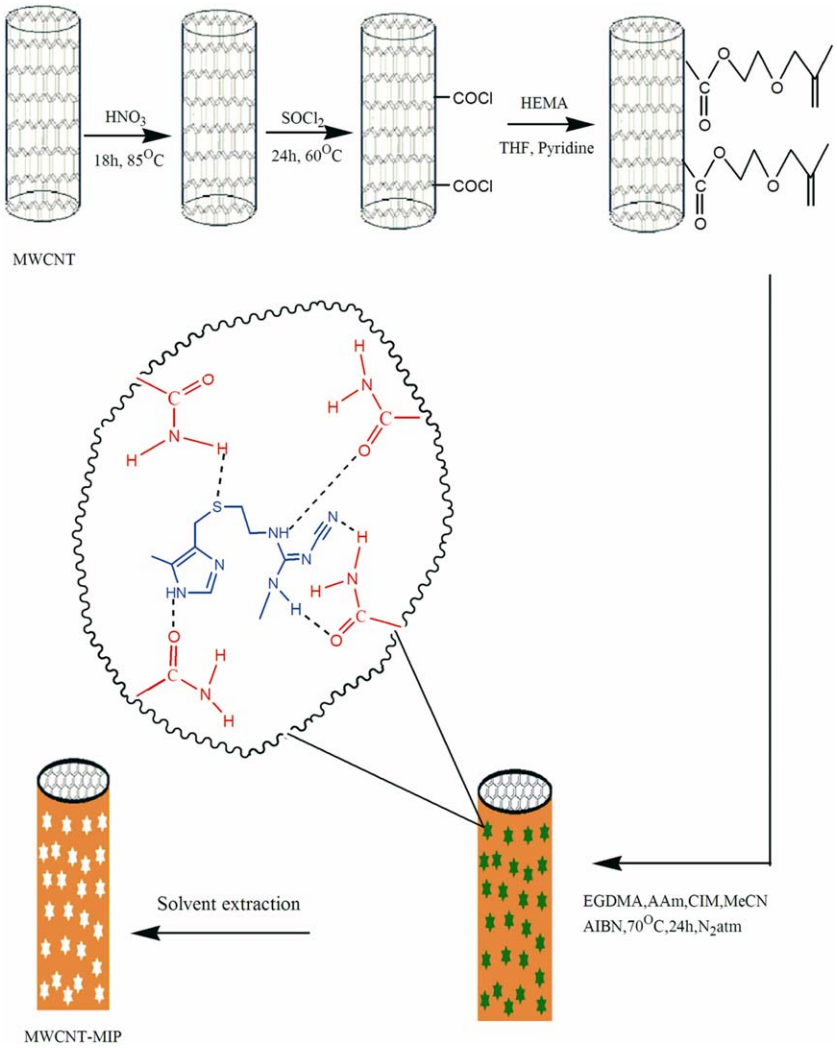

Figure 1. Synthesis route of MWCNT-MIP. [Color figure can be viewed in the online issue, which is available at wileyonlinelibrary.com.]

capacity (Q_e) of the adsorbent was calculated [eq. (1)]. The theoretical adsorption capacity value for the adsorbent was also calculated using the Langmuir [eq. (2)] and Freundlich [eq. (3)] equations:

$$(1/Q_e)=(1/Q_m)+(1/Q_mK_a)\times(1/C_e) \quad (2)$$

$$\log(Q_e)=\log K_F+ 1/n \log C_e \quad (3)$$

where C_e (mmol L^{-1}) and Q_e (mmol g^{-1}) are CIM concentration and amount adsorbed at adsorption equilibrium, Q_m (mmol g^{-1}) and K_a (L mg^{-1}) are the theoretical maximum adsorption capacity and Langmuir equilibrium constant related to the theoretical maximum adsorption capacity and energy of adsorption, respectively. K_F and n are the Freundlich constants, which denote the adsorption capacity and adsorption intensity, respectively. All parameters of each model can be found from the slope and intercept of the different plots using regression analysis. The validity of isotherm models was compared by using correlation coefficient (R^2) value.

Table I. Preparation of Imprinted and Nonimprinted Polymers with and Without MWCNT

Sorbents	AAm (mmol)	EGDMA (mmol)	CIM (mmol)	AIBN (mg)	MWCNT—CH=CH_2 (mg)
MWCNT MIP	0.5	1	0.1	50	75
MWCNT NIP	0.5	1	-	50	75
MIP	0.5	1	0.1	50	-
NIP	0.5	1	-	50	-

Kinetic Studies

The kinetic parameters of the systems were studied using batch equilibration process. About 10 mg of MWCNT-MIP was treated with a number of 8 mL samples of 2.4 mmol L^{-1} CIM solution. After equilibration at different time intervals, the mixture was centrifuged (1600 rpm), filtered and the concentration of CIM in the supernatant was measured at 220 nm using a UV–vis spectrophotometer. The adsorption amount bound at different time intervals was calculated using eq. (1).

The desorption kinetics was studied using the Langergren kinetic model. The values were plotted for first-order [eq. (4)] and second-order [eq. (5)] kinetics represented as:

$$\ln (Q_e - Q_t) = \ln \; Q_e - k_1 t \tag{4}$$

$$(t/Q_t) = \left(1/k_2 Q^2{}_e\right) + (t/Q_e) \tag{5}$$

where Q_e (mmol g^{-1}) and Q_t (mmol g^{-1}) are the amount of template bound at equilibrium and at time t respectively, t (min) is any given time and k_1 (min^{-1}) and k_2 (g $mmol^{-1}min^{-1}$) are first-order and second-order rate constants, respectively. From the plots $\ln(Q_e - Q_t)$ vs t and t/Q_t vs t the values Q_e, k_1, and k_2 were calculated.

Selectivity Studies

The selective adsorption of CIM over its structural analogues RAN and FAM by the sorbents was done using batch equilibration process where 2.4 mmol solutions of CIM, RAN, and FAM were used. The procedure was same as that of adsorption studies. The extent of selectivity was found to depend on the number and complimentarity of the imprinted cavities and also their rebinding ability. This effect was calculated using the following equation:

$$K_d = (C_i - C_f) V / M C_f \tag{6}$$

where K_d (L g^{-1}) is the distribution coefficient, C_i (mmol L^{-1}) and C_f (mmol L^{-1}) are the initial and final solution concentrations, respectively, and M (g), the mass of the sorbent used.

The selectivity coefficient (k) and relative selectivity coefficients (k') were determined using the following equations:

$$k = K_{\text{template}} / K_{\text{analogue}} \tag{7}$$

$$k' = K_{\text{MIP}} / K_{\text{NIP}} \tag{8}$$

Reusability

The CIM adsorption and desorption study was repeated 10 times using the same polymer for testing its reusability under the same conditions. For this purpose, 10 mg each of MWCNT-MIP and bulk MIP polymers were weighed and incubated in a solution of CIM having 2.4 mmol L^{-1} concentration. After 4 h of incubation, the polymers were centrifuged and the amount of unbound CIM was analyzed by UV–visible spectroscopy. Then the polymers were washed with acetonitrile and dried under vacuum for the next application.

RESULTS AND DISCUSSION

FTIR spectra were used to characterize the structural changes of all intermediates and products formed during the synthesis of MWCNT-MIP. Figure 2 shows the FTIR spectra of purified MWCNT, MWCNT-COOH, MWCNT-CH═CH_2, and MWCNT-MIP before and after washing. In the spectrum of purified MWCNT (a), a strong peak at 1737 cm^{-1} is in correspondence to the C═O stretching vibration, whereas the peak at 2928 cm^{-1} is related to the asymmetric stretching vibration of C—H. New peaks at 3300 and 1581 cm^{-1} for the acid processed MWCNTs can be found in spectrum (b), which confirmed the presence of functional groups —OH and —COOH. The peak at 1352 cm^{-1} and several low intensity peaks could be attributed to the C—O stretching vibrations of the —COOH. In spectrum (c) a strong peak associated with ether linkage around 1166 cm^{-1} was observed. The presence of this peak suggests that HEMA is coupled to MWCNT through the —O— atom. The 1630 cm^{-1} peak of C═C, characteristic of HEMA is also present, indicating that the C═C bond is formed after the coupling reaction. MWCNT-MIP before and after washing gave a notable change in spectra such as the additional peaks at 3136 and 3216 cm^{-1} for N—H stretch and at 2176 and 1615 cm^{-1} for —CN triple bond and >C═N— stretch of cyano-guanidine unit of CIM in the before washing spectrum of MWCNT-MIP indicating the embedding of CIM within the polymer.

The X-ray diffraction technique was used to determine the crystallinity of MWCNT-MIPs (Figure 3). The XRD pattern of MWCNT shows two crystalline peaks at $2\theta = 25.8°$ and $2\theta = 43.7°$ corresponding to the interlayer spacing (d_{002}) and reflection (d_{100}) of MWCNT.[17] The acid-functionalized carbon nanotubes were found to retain the crystalline nature. The conventional MIPs scatter the X-ray beams to give a very broad peak ($2\theta = 15°$) characteristic of its amorphous nature, while MWCNT-MIPs show sharp peaks imparted by the MWCNTs in addition to peaks of bulk MIPs; but with less intensity. This indicates the effective clubbing of the nanostructures into the polymer matrix.

To study the differences in thermal behavior of MWCNTs, MWCNT-MIPs, and bulk MIPs, TG analysis was done (Figure 4). Pristine MWCNT was found to be thermally stable up to 800°C without any substantial mass loss. Thermal decomposition pattern of MWCNT-COOH was obtained with a continuous but not obvious mass loss because of the rupturing of carbonyl groups from the surface of MWCNT. From the residual yield, the percentage of acid formation on the surface of carbon nanotubes was found to be 8%. Thermogram of MWCNT-MIP showed a similar profile to that of pure MIP. However, the decomposition temperature and mass loss were lower and higher, respectively, for MIP in comparison with MWCNT-MIP which implies the greater thermal stability induced to the MWCNT-MIP because of the incorporation of MWCNTs. From the residual mass, percentage of multiwalled carbon nanotube in MWCNT-MIP was found to be about 12%.

The SEM micrographs of pristine MWCNT showed nanosized tubular moieties with an average diameter around 6–8 nm. Functionalized MWCNTs showed a slight increase in diameter with the retainment of morphology. Both the MIPs showed more rough surface morphologies in comparison with NIPs because of the leaching out of print molecules from the polymer matrix. Further, conventional MIPs exhibited a sponge-like agglomerated morphology which was dramatically changed into

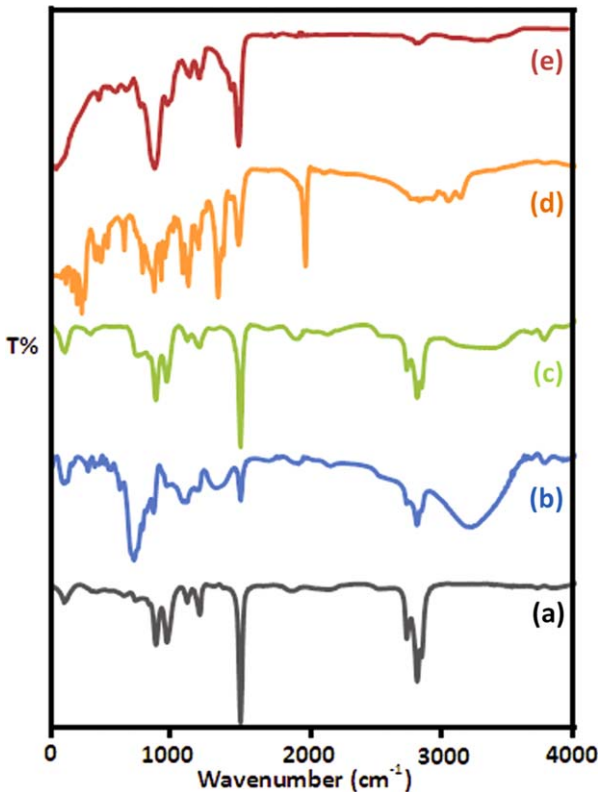

Figure 2. FTIR spectra of (a) purified MWCNT, (b) MWCNT-COOH, (c) MWCNT-CH_2=CH_2, (d) MWCNT-MIP before washing, and (e) after washing. [Color figure can be viewed in the online issue, which is available at wileyonlinelibrary.com.]

tubular forms on the incorporation of MWCNTs into the polymer matrix (Figure 5).

For a more detailed morphological analysis, HR-TEM was taken. Pure MWCNTs showed nanotubes with a diameter ranging from 6 to 8 nm and an approximate length of some micrometers (Figure 6). On polymerization, the thickness of the nanotubes was found to increase to about 24–27 nm although it retained its nanofibrillar morphology which clearly indicates that the polymer was effectively wrapped around the carbon nanotubes thereby providing with the binding cavities on its surface. On the other hand, the bulk MIPs showed some agglomerated bundle-like structures with possibly more cavities in the bulk. This also substantiates the higher homogeneity expressed by the MWCNT-polymer system.

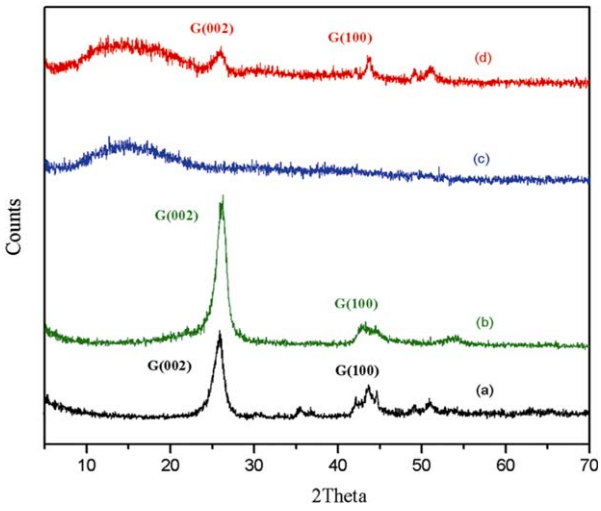

Figure 3. Powder X-ray diffraction patterns of (a) MWCNT, (b) MWCNT-COOH, (c) MIP, and (d) MWCNT-MIP. [Color figure can be viewed in the online issue, which is available at wileyonlinelibrary.com.]

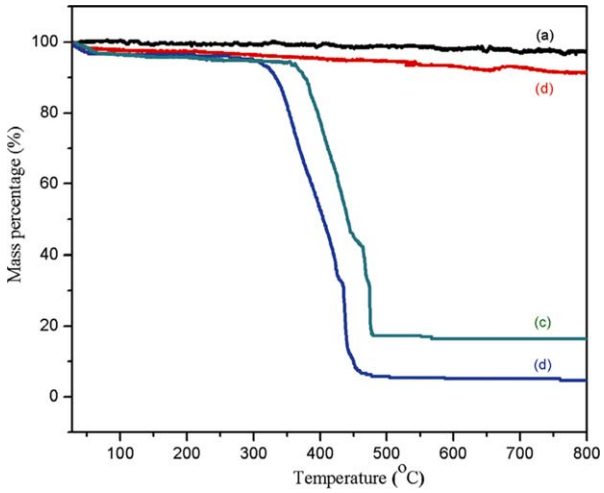

Figure 4. TGA curves of (a) MWCNT, (b) MWCNT-COOH, (c) MWCNT-MIP, and (d) MIP (heating rate of 10°C min^{-1} from room temperature to 800°C under N_2 atmosphere). [Color figure can be viewed in the online issue, which is available at wileyonlinelibrary.com.]

Concentration Study

The effect of initial template concentration in the range of 0.4–3.6 mmol L^{-1} on adsorption (investigated under the specified conditions; contact time of 4 h; adsorbent dosage of 10 mg; and temperature of 28°C) is shown in Figure 7. To compare the capacity of adsorption, bulk MIP and MIPs formed at the surface of the nanomaterials (MWCNTs) were chosen. As can be seen, no difference in the adsorbance Q_e of CIM for MWCNT-MIP and MIP could be observed when the template concentration was less than 0.05 mmol L^{-1} whereas an obvious difference could be found when the concentration of CIM was above 0.4 mmol L^{-1}. It might be that the different adsorbance Q_e of CIM between MWCNT-MIP and MIP was caused by the different quantity of available binding sites. At lower CIM concentration, the template quantity was not enough to saturate all the binding sites of the MWCNT-MIP or MIP, resulting in no difference in their adsorbance. However, when CIM was saturated, the presence of more number of specific binding cavities on the surface of MWCNT-MIPs became evident. It was observed that the adsorption capacity increased from 0.2569 to 0.4147 mmol g^{-1} for MWCNT-MIP and from 0.09414 to 0.2831 mmol g^{-1} for MIP with an increase in initial template concentration and the adsorption capacity of the polymer on MWCNTs was 31.73% higher than that of the imprinted bulk polymer. It might be attributed to the fact that the incorporation of high surface-to-volume ratio nanostructures into the polymer matrix results in increased solid–liquid surface of contact thereby

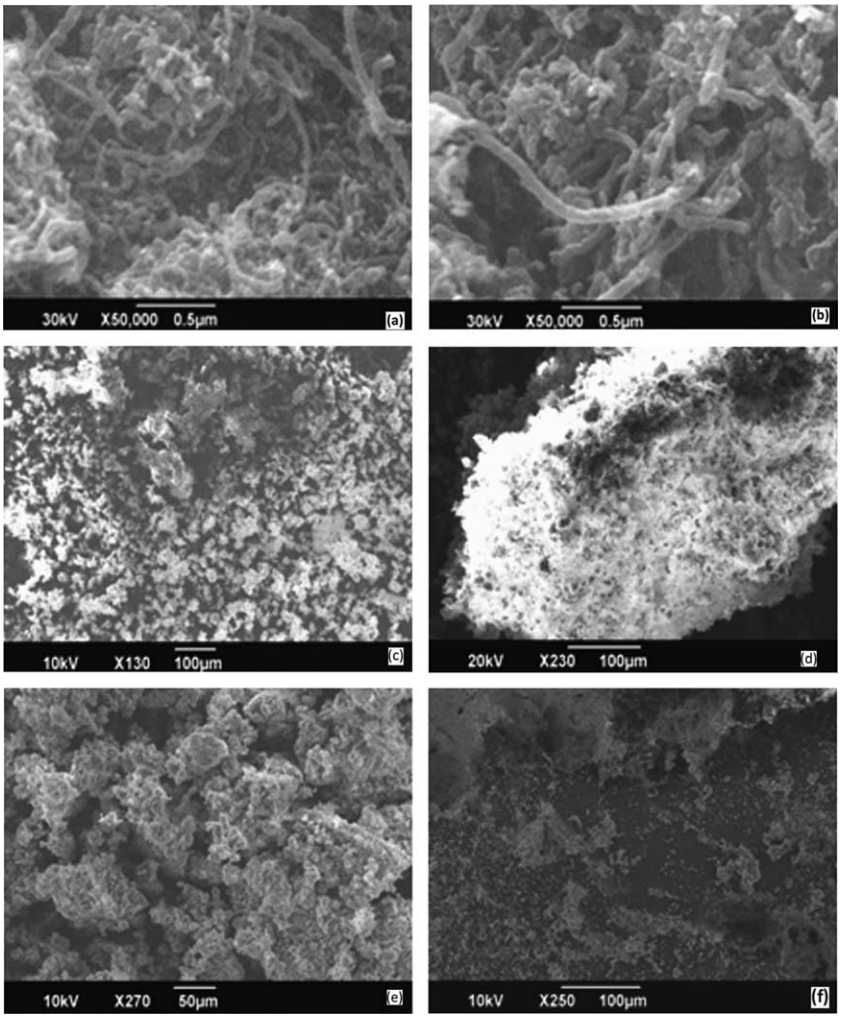

Figure 5. Scanning electron micrographs of (a) MWCNT, (b) MWCNT-COOH, (c) MWCNT-MIP, (d) MWCNT-NIP, (e) MIP, and (f) NIP.

providing more accessible binding sites and higher valid collisions between MWCNT-MIP and template. Also, the increased affinity of the imprinted polymers towards the template molecule as compared to the nonimprinted polymers revealed that they had recognition ability for CIM, which could be ascribed to the formation of complementary cavities. The noncovalent forces, associated with cavity conformations, were the main cause for the affinity and specificity of MIPs to the template.

Adsorbent Dosage

The influence of imprinted polymer adsorbent dosage on CIM sorption was examined by varying dosages from 5 to 20 mg. Figure 8 presents typical set of results obtained by varying adsorbent dosages during template sorption. From the analysis of experimental data obtained, it was observed that the removal efficiency increased with increase in sorbent dosage owing to the increase in number of binding sites. The increase in effectiveness of adsorption with adsorbent dose was maximal for MWCNT-MIP which may be because of the increase in surface-to-volume ratio. Both the NIPs showed a much less marked difference in the amount adsorbed because of the absence of specific binding sites.

Adsorption Isotherms

Equilibrium data, commonly referred to as adsorption isotherms, are basic requirements for the designing of adsorption systems. The adsorption isotherms represent the relationship between the amount adsorbed by unit weight of adsorbent and the amount of adsorbate remaining in the solution at equilibrium. The Langmuir isotherm model assumes a monolayer adsorption onto a surface containing a finite number of adsorption sites of uniform strategies of adsorption with no transmigration of adsorbate in the plane of surface. Based on the least square fit, adsorption isotherm data of MWCNT-MIP were well fit with the Langmuir model than that for MIP (Figure 9). As illustrated in the figure, a linear plot with correlation coefficient (R^2) value of 0.998 was obtained from Langmuir isotherm equation for MWCNT-MIP when plotting $1/C_e$ against $1/Q_e$ with a slope and intercept equal to $1/Q_mK_a$ and $1/Q_m$, respectively. Consequently, adsorption isotherm data provided that the adsorption process was mainly monolayer on a homogeneous

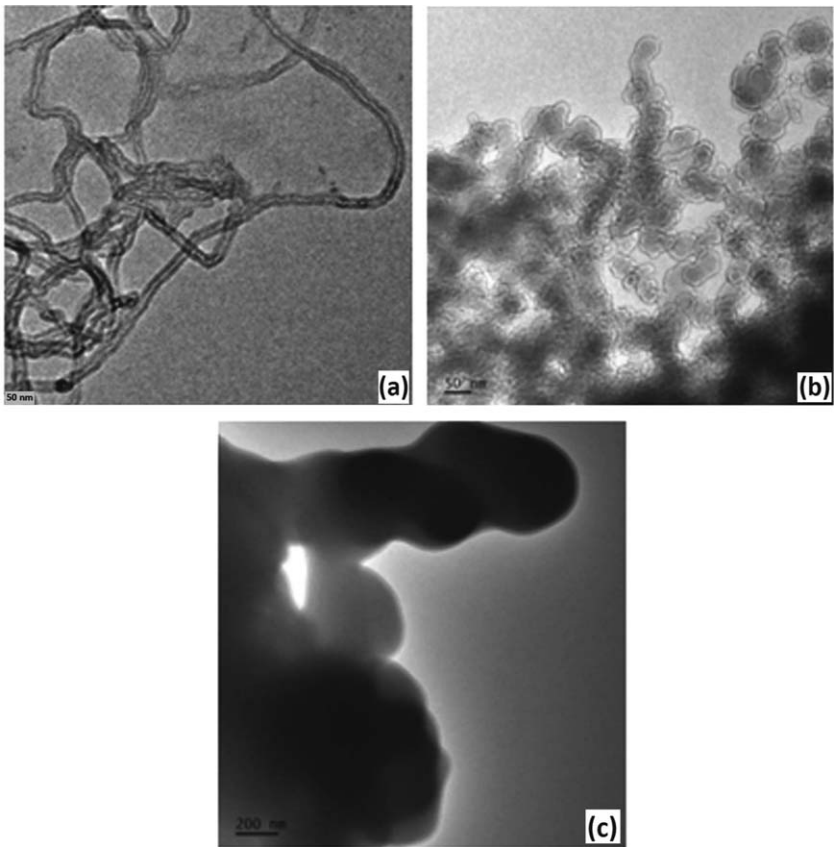

Figure 6. TEM Images of (a) MWCNT, (b) MWCNT-MIP, and (c) MIP.

adsorbent surface. The Langmuir constants Q_m and K_a were found to be 0.4199 mmol g^{-1} and 0.1194 L $mmol^{-1}$, respectively. It is also interesting to note that the CIM adsorption capacity calculated from Langmuir equation (0.4199 mmol g^{-1}) was closely associated with that experimentally obtained (0.4147 mmol g^{-1}) from the isotherm study. Figure 9 shows an L type profile according to Giles et al.'s classification,[18] reflecting a strong attraction between CIM and MWCNT-MIP.

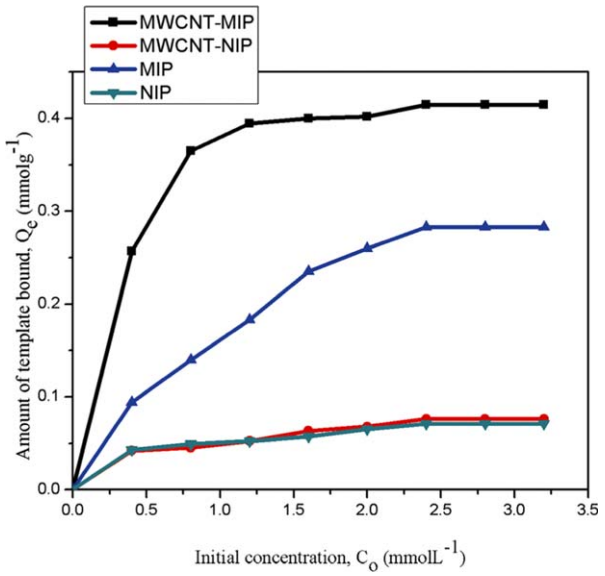

Figure 7. Adsorption isotherms of imprinted and nonimprinted polymers (Amount of polymer, 10 mg; volume, 8.0 mL; concentration of CIM from 0.4 to 3.6 mmol L^{-1}). [Color figure can be viewed in the online issue, which is available at wileyonlinelibrary.com.]

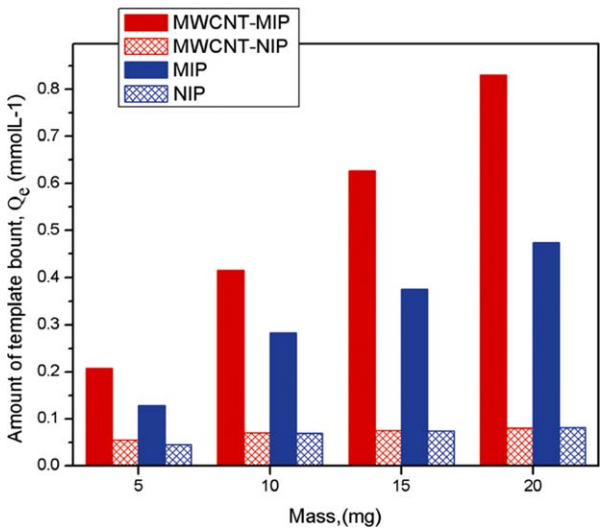

Figure 8. Effect of adsorbent dosage on template bound (Amount of polymer varies from 5 to 20 mg; volume, 8.0 mL; concentration of CIM, 2.4 mmol L^{-1}, binding time, 3 h). [Color figure can be viewed in the online issue, which is available at wileyonlinelibrary.com.]

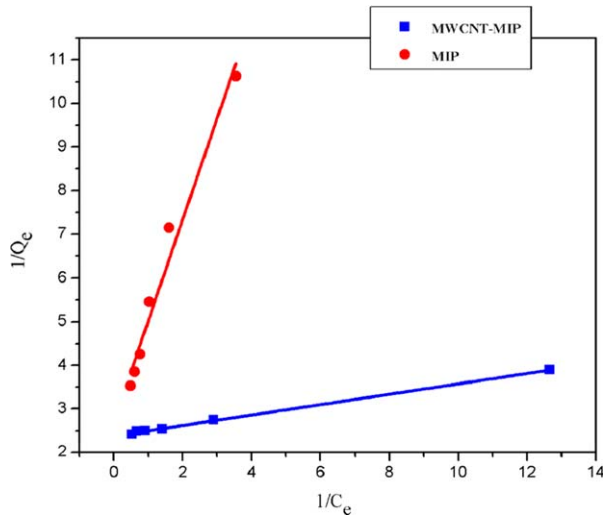

Figure 9. Langmuir plot for adsorption of CIM by MWCNT-MIP and MIP (Amount of polymer 10 mg; volume, 8.0 mL; concentration of CIM 0.4 to 2.4 mmol L^{-1}, binding time, 3 h). [Color figure can be viewed in the online issue, which is available at wileyonlinelibrary.com.]

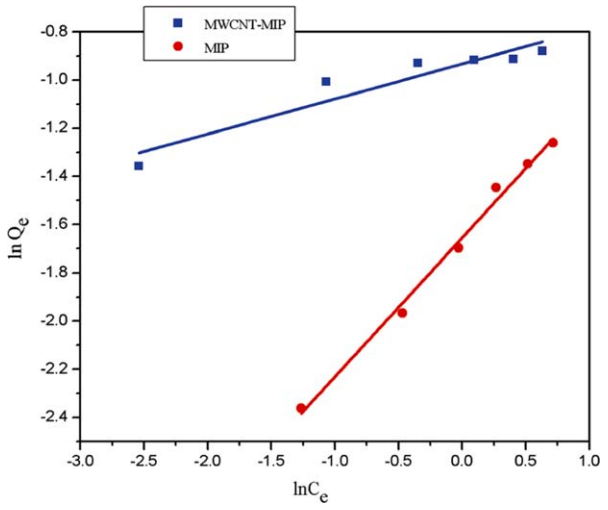

Figure 10. Freundlich plot for adsorption of CIM by MWCNT-MIP and MIP (Amount of polymer 10 mg; volume, 8.0 mL; concentration of CIM 0.4–2.4 mmol L^{-1}, binding time, 3 h). [Color figure can be viewed in the online issue, which is available at wileyonlinelibrary.com.]

Freundlich adsorption isotherm is an empirical one for nonideal adsorption on heterogeneous surfaces as well as for multilayer adsorption. The equilibrium data were further analyzed using the linearized form of Freundlich isotherm by plotting ln Q_e versus ln C_e, as shown in Figure 10. The calculated Freundlich isotherm constants and the corresponding correlation coefficients for MWCNT-MIP and MIP are shown in Table II. From the data, it can be concluded that the Langmuir isotherm model was more suitable for the experimental data of MWCNT-MIP than Freundlich isotherm because of the high value of the correlation coefficient, suggesting that adsorption takes place at specific homogeneous sites and no further adsorption takes place at the site which has been already occupied by a template molecule. In the case of MWCNT-MIP the theoretical and experimental values of the Freundlich isotherm show a large deviation while those for the Langmuir isotherm do not.

Adsorption Kinetics

So as to further expose the rate-controlling steps and sorption mechanism of CIM onto MWCNT-MIP, a kinetic investigation was conducted. Pseudo-first and pseudo-second-order equations have been used for testing experimental data. The rate of adsorption of CIM by the MWCNT-MIP was measured as a function of time. Figure 11 shows the dynamic curve of the adsorption of CIM onto the MWCNT-MIPs at 2.4 mmol L^{-1} concentration of CIM. The sorption process was rapid in the initial stage and rather slow when approaching equilibrium. The results show that the rapid adsorption of CIM occurred onto the surface recognition sites of the MWCNT-MIPs. When the imprinted sites on the MWCNT-MIP were occupied, the adsorption rate of CIM decreased. The maximum adsorption occurred after 1.5 h at a capacity around 0.4011 mmol L^{-1}. The sorption kinetic data were analyzed using the Langergen first-order rate model.[19] The equations involved are as below:

$$dQ_t/d_t = k_1(\ Q_e - Q) \tag{9}$$

where k_1 (min^{-1}) is the rate constant of pseudo-first-order sorption, Q_t denotes the amount of CIM sorption (mmol g^{-1}) at time t (min) and Q_e denotes the amount of CIM adsorption (mmol g^{-1}) at equilibrium. After definite integration and applying the initial conditions $Q_t = 0$ at $t = 0$ and $Q_t = Q_t$ at $t = t$, eq. (1) becomes

$$\ln(Q_e - Q_t) = \ln(Q_e) - k_1 t \tag{10}$$

In addition, a pseudo-second-order equation proposed by Ho and McKay[20] based on the assumption that the adsorption follows chemisorption may be expressed in the form:

$$\mathrm{d}Q_t/d_t = k_2(Q_e - Q)^2 \tag{11}$$

where k_2 is the rate constant of pseudo-second-order sorption. Integrating Eq. (3) and applying the initial conditions

$$1/(Q_e - Q_t) = (1/Q_e) + k_2 t \tag{12}$$

or equivalently

$$(t/Q_t) = \left(1/k_2 Q_e^2\right) + t/Q_e \tag{13}$$

Table II. Adsorption Isotherm Parameters of MWCNT-MIP and MIP

	Langmuir parameters			Freundlich parameters		
Sample	Q_m (mmol g^{-1})	k_a (L $mmol^{-1}$)	R^2	n	k_f [(mmol/g)(L/mmol)$^{1/n}$]	R^2
MWCNT-MIP	0.369	1.027	0.998	1.736	0.394	0.882
MIP	0.419	2.034	0.966	6.863	0.191	0.991

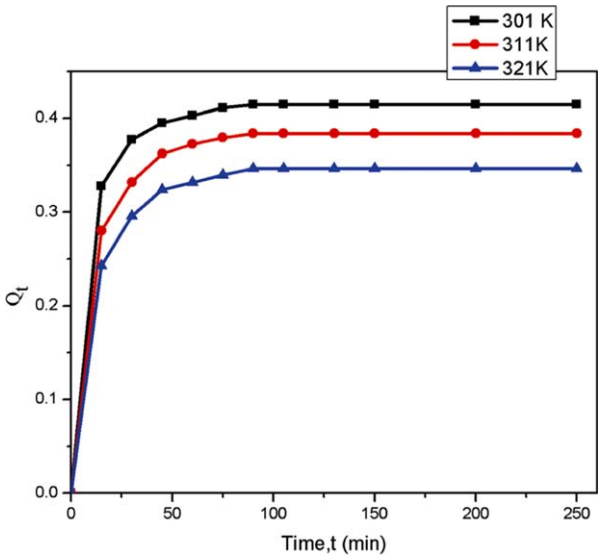

Figure 11. Adsorption rate of CIM by MWCNT-MIP (Amount of polymer 10 mg; volume, 8.0 mL; concentration of CIM 0.4–2.4 mmol L^{-1}, binding time, 3 h, temperature ranging from 301 to 321 K). [Color figure can be viewed in the online issue, which is available at wileyonlinelibrary.com.]

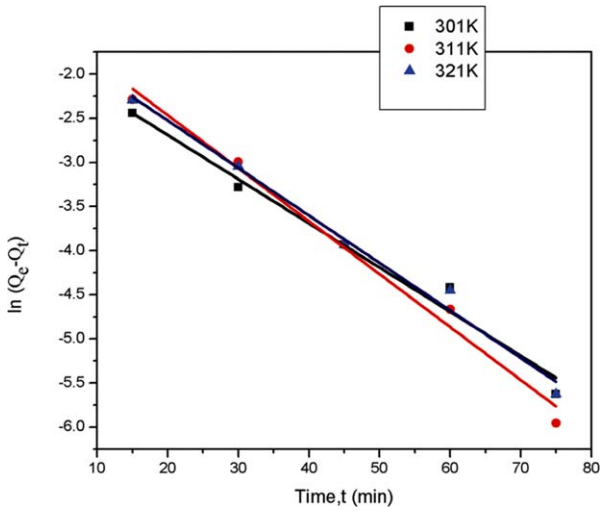

Figure 12. Pseudo-first-order kinetic plot for adsorption of CIM by MWCNT-MIP (Amount of polymer 10 mg; volume, 8.0 mL; concentration of CIM 2.4 mmol L^{-1}, binding time, 3 h, temperature ranging from 301 to 321 K). [Color figure can be viewed in the online issue, which is available at wileyonlinelibrary.com.]

The constants were determined experimentally by plotting $\ln(Q_e - Q_t)$ versus t (Figure 12) and listed in Table III. The data does not fall on a straight line and had a low correlation coefficient, indicating the first order kinetic model is less appropriate. The theoretic values (Q_e,cal) are far lower than those from experimental data, (Q_e,exp) (Table III), again implying that the adsorption process does not follow fully the pseudo-first-order adsorption rate expression. The plot t/Q_t versus t ought to give a straight line if second order kinetics is applicable and the values Q_e and k_2 can be calculated from the slope and the intercept of the plot, respectively. Further, the plot of t/Q_t against t resulted in a high correlation coefficient (0.999) (Figure 13). This indicates that CIM adsorption by MWCNT-MIP follows a second-order kinetics. When the temperature was increased, values of kinetic parameters (k and Q_e) were decreased showing that the adsorption process was exothermic (Table III). When the temperature of the reaction was increased the adsorption was decreased and desorption of the template molecule from the adsorption site was increased at higher temperature.[21]

Selectivity Experiments

To check the selectivity of MWCNT-MIP and bulk MIP towards the CIM molecule, in addition to the template CIM two other structurally similar compounds RAN and FAM were selected as interfering substrates (Figure 14). The binding capacities of the MWCNT-MIP, MIP, and nonimprinted polymers of both sorbents are shown in Figure 15. MWCNT-MIP showed maximum binding capacity for CIM molecule compared with bulk MIP because of the increased number of binding sites in the surface of the nanostructured MIP. The adsorption efficiency of NIPs for CIM was lower than that of both MIPs whereas the adsorption capacities of all the four sorbents were found to be more or less same for the structural analogs RAN and FAM. These results suggested that the molecular imprinting process created a micro-environment depending on the interaction, size, shape, and functionality of the template.[22] There were no proper cavities and recognition sites formed in the NIP, so that it binds compounds only by nonspecific adsorption[23] which led to its decreased adsorption capacity than the MIPs. Also, because of the lack of structure specific cavities there was no significant difference in adsorption efficiency for the interfering compounds. Table IV summarizes the distribution coefficient (K_d), selectivity coefficient (k), and relative selectivity coefficient (k').

Regeneration and Robustness

The regeneration of MWCNT-MIP/MIP was investigated in ten sequential cycles of adsorption–desorption. After incorporation

Table III. Kinetic Parameters of the Pseudo-First-Order and Pseudo-Second-Order Equations for CIM Adsorption onto MWCNT-MIP

			Pseudo-first order			Pseudo-second order		
C_o (mmol L^{-1})	Temperature (K)	$Q_{e,\ exp}$	$Q_{e,\ cal}$ (mmol g^{-1})	K_1 (min^{-1})	R^2	$Q_{e,\ cal}$ (mmol g^{-1})	K_2 ($gmmol^{-1}min^{-1}$)	R^2
2.4	301	0.415	0.185	0.050	0.973	0.421	0.742	0.999
2.4	311	0.383	0.282	0.060	0.984	0.392	0.689	0.999
2.4	321	0.343	0.235	0.053	0.984	0.355	0.643	0.999

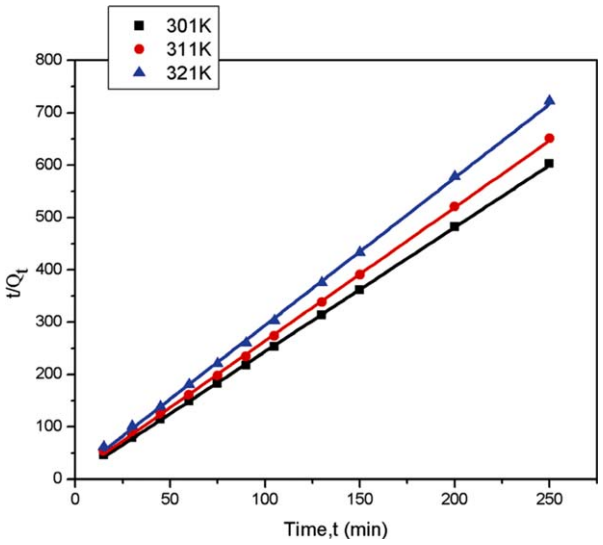

Figure 13. Pseudo-second-order kinetic plot for adsorption of CIM by MWCNT-MIP (Amount of polymer 10 mg; volume, 8.0 mL; concentration of CIM 2.4 mmol L^{-1}, binding time, 3 h, temperature ranging from 301 to 321 K). [Color figure can be viewed in the online issue, which is available at wileyonlinelibrary.com.]

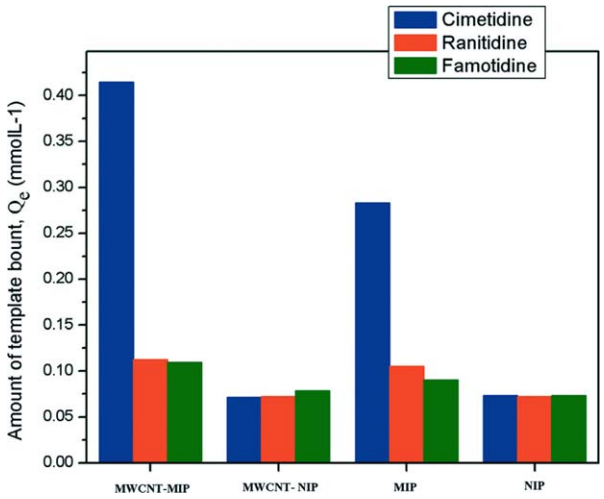

Figure 15. Evaluation of the selectivity of the MWCNT-MIP compared with MIP and both the NIPs for CIM, RAN, and FAM at wavelengths of 220, 228, and 211 nm, respectively. [Color figure can be viewed in the online issue, which is available at wileyonlinelibrary.com.]

of CIM onto the imprinted sorbents, the MIPs were regenerated using the porogen acetonitrile. Figure 16 shows the adsorption efficiency of both the MIPs for CIM in 10 consecutive adsorption-regeneration cycles. The experiment showed that the MWCNT-MIP showed 100% adsorption-regeneration up to five cycles. After that the regeneration capacity slightly decreased but not obviously which may be attributed to the destruction of some recognition sites in the network of CNT-MIP during the time of rewashing, and thus, were not fit for the template molecule anymore. The bulk MIP showed irregular trends of regeneration from the second cycles onwards because in addition to the destruction of some recognition sites, it is very difficult to leach out the entire template from the bulk during the regeneration process. So MWCNT-MIP is a better adsorbent for selective recognition and separation of CIM from its structural analogues than the bulk MIP.

Table IV. The Distribution Coefficient (K_d), Selectivity Coefficient (k), and Relative Selectivity Coefficient (k') of MWCNT-MIP and MIP

Sample	Drugs	Q_e	K_d	k	k'
MWCNT-MIP	CIM	0.4147	0.2204	-	6.824529
	RAN	0.1124	0.0498	4.326692	1.577309
	FAM	0.1096	0.0484	4.817444	1.416629
MWCNT-NIP	CIM	0.0713	0.0309	-	-
	RAN	0.0725	0.0314	-	-
	FAM	0.0784	0.0341	-	-
MIP	CIM	0.2831	0.1384	-	4.234596
	RAN	0.1048	0.0462	2.871809	1.47454
	FAM	0.0906	0.0396	3.399154	1.245779
NIP	CIM	0.0735	0.0318	-	-
	RAN	0.0721	0.0312	-	-
	FAM	0.0733	0.0317	-	-

CONCLUSIONS

In this work, a molecular imprinted nano-structured sorbent for selective recognition of CIM from its structural analogues was constructed. The parameters such as effect of template concentration, adsorbent dose, contact time, and temperature on the adsorption of CIM by the synthesized sorbents were optimized and compared. Maximum adsorption capacity was 31.73% increased after the incorporation of MWCNT onto MIPs. The rate of kinetics of CIM adsorption was rapid in the case of MWCNT-MIP than the bulk MIP. MWCNT-MIP showed exothermic adsorption process. The adsorption isotherms were well fitted to the Langmuir isotherm model which ensures homogeneous distribution of binding sites within the MWCNT-MIP matrix. The selectivity experiments showed that the MWCNT-MIP had higher adsorption capacities for CIM than for its structural analogue molecules, RAN and FAM.

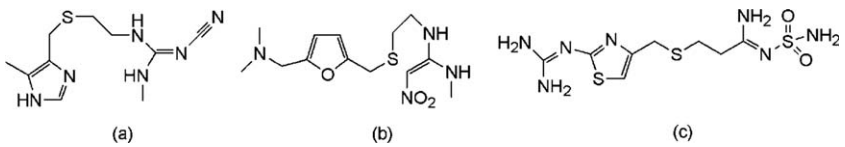

Figure 14. Chemical structures of (a) CIM, (b) RAN, and (c) FAM.

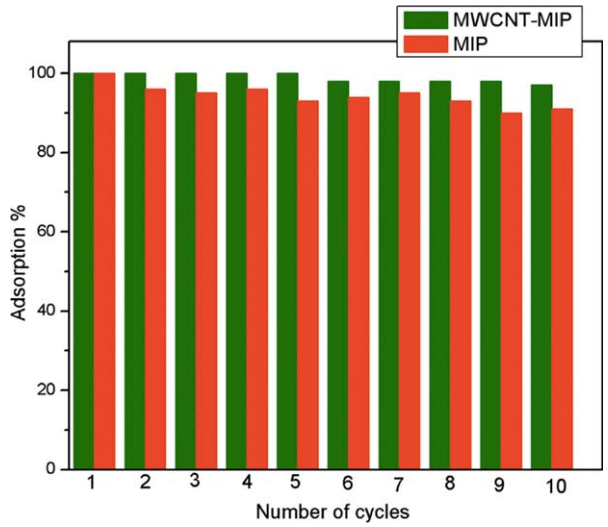

Figure 16. Regeneration cycles of CIM onto MWCNT-MIP and MIP using acetonitrile as desorbing agent (Amount of polymer 10 mg; volume, 8.0 mL; concentration of CIM 2.4 mmol L^{-1}, binding time, 3 h). [Color figure can be viewed in the online issue, which is available at wileyonlinelibrary.com.]

ACKNOWLEDGMENTS

One of the authors (SMP) would like to thank University Grants Commission (UGC) for the financial assistance awarded as Rajiv Gandhi National Fellowship (RGNF).

AUTHORSHIP NOTE

SMP has done the acquisition, analysis and interpretation of data and drafting of the full paper. BM is the guide and corresponding author.

REFERENCES

1. Shea, K. J.; Sasak, D. Y. *J. Am. Chem. Soc.* **1989**, *11*, 3442.
2. Arshady, R.; Mosbach, K. *Makromol. Chem.* **1981**, *182*, 687.
3. Suedee, R. *Pharm. Anal. Acta* **2013**, *4*, 264.
4. Nicholas, W. T.; Christopher, W. J.; Keith, R. B.; Christopher, J. A.; Vladimir, H.; David, W. B. *Biotechnol. Prog.* **2006**, *22*, 1474.
5. Pan, J. M.; Yao, H.; Xu, L. C.; Ou, H. X.; Huo, P. W.; Li, X. X.; Yan, Y. S. *J. Phys. Chem. C.* **2011**, *115*, 5440.
6. Anirudhan, T. S.; Sheeba, A. *J. Chem. Technol. Biotechnol.* **2013**, *88*, 1847.
7. Haisheng, Z.; Weiping, Z.; Hongqing, W.; Yuyuan, W.; Fangfang, H.; Zhiqiang, C.; Honglin, L.; Jinhui, T. *J. Anal. Sci.; Methods Instrum.* **2012**, *2*, 60.
8. Xianwen, K.; Tingting, L.; Chen, Li.; Hong, Z.; Zonglan, X.; Anhong, Z. *J. Solid State Electrochem.* **2012**, *16*, 3207.
9. Mohammad, B. G.; Maryam, T. *Talanta.* **2011**, *84*, 905.
10. Francesco, P.; Silke, H.; Ortensia ilaria, P.; Abdelwahab, H.; Giuseppe, C.; Nevio, P. *J. Appl. Polym. Sci.* **2013**, *130*, 829.
11. Guoyong, X.; Wei-Tai, W.; Yusong, W.; Wenmin, P.; Pinghua, W.; Qingren, Z.; Fei, L. *Nanotechnology* **2006**, *17*, 2458.
12. Devkar, S. R.; Salunkhe, V. R. *Int. J. Pharm. Technol.* **2013**, *5*, 5257.
13. Hayashi, A.; Kobayashi, K.; Imaeda, Y.; Matsumoto, S. *Gan to Kagaku Ryoho.* **2003**, *30*, 1788.
14. Jianfeng, S.; Yizhe, H.; Chen, Q.; Mingxin, Y. *Langmuir* **2008**, *24*, 3993.
15. Boehm, H. P. *Carbon* **1994**, *32*, 759.
16. Nanjundan, A. K.; Hullathy, S. G.; Jong, S. K.; Yong S. J.; Yeon, T. *J. Eur. Polym. J.* **2008**, *44*, 579.
17. Van der Lee, M. K.; Van Dillen, A. J.; Bitter, J. H.; De Jong, K. P. *J. Am. Chem. Soc.* **2005**, *127*, 13573.
18. Giles, C. H.; McEwen, T. H.; Nakhwa, S. N.; Smith, D. *J. Chem. Soc.* **1960**, *4*, 3973.
19. Lagergren, S. K. *Sven. Vetenskapsakad. Handl*, **1898**, *24*, 1.
20. Ho, Y. S.; McKay, G. *Can. J. Chem. Eng.* **1998**, *76*, 822.
21. Jnr, M. H.; Spiff, A. I. *Electron. J. Biotechnol.* **2005**, *8*, 162.
22. Ying, L.; Xin, Li.; Cunku, D.; Yuqi, L.; Pengfei, J.; Jingyao, Q. *Biosens. Bioelectron.* **2009**, *25*, 306.
23. Le, N. M.; Plieva, F.; Hey, T.; Guieysse, B.; Mattiasson, B. *J. Chromatogr. A*, **2007**, *1154*, 158.